Encapsulation of resveratrol using Maillard conjugates and membrane emulsification

Encapsulation of resveratrol using Maillard conjugates and membrane emulsification

> ⓘ The corrections made in this section will be reviewed and approved by a journal production editor.

Larissa Consoli Visualization Writing - original draft Data curation Formal analysis Investigation Conceptualization [a,b,*] larissa.consoli@gmail.com, Míriam Dupas Hubinger Funding acquisition Writing - review & editing Supervision [a], Marijana M. Dragosavac Writing - review & editing Supervision Resources Methodology Conceptualization [b]

[a]School of Food Engineering, University of Campinas, Campinas, São Paulo, Brazil

[b]Chemical Engineering Department, Loughborough University, Loughborough, Leicestershire, United Kingdom

*Corresponding author at: School of Food Engineering, University of Campinas, Campinas, São Paulo, Brazil.

Abstract

Resveratrol is a stilbene phenolic associated with health-promoting properties such as antioxidant, anti-inflammatory and chemoprevention. Due to its chemical instability and low water solubility, microencapsulation represents a good alternative to provide better results when employing resveratrol as a nutraceutical ingredient. The main purpose of our work was to use low shear membrane emulsification to produce resveratrol-loaded emulsions of low polydispersity and integrate this process to spray drying to produce a powdered product. Resveratrol was dispersed with palm oil in a continuous phase obtained via Maillard reaction. We evaluated the influence of process conditions and phases composition on emulsions properties and performed the characterization of the spray-dried powder. Emulsions droplet size and span decreased as shear stress was increased. Higher dispersed phase fluxes provided increased droplet size polydispersity. Process conditions were set on 60.0 Pa shear stress and 70 L $m^{-2}h^{-1}$ of dispersed phase flux, obtaining emulsions with mean diameter around 30 μm and span of 0.76. Despite this relatively high droplet size of the infeed emulsions, the spray drying process resulted in particles with high encapsulation efficiency (97.97 ± 0.01%), and water content (~3.6%) and diameter (~10.2 μm) similar to particles obtained from fine emulsions in previously reported works.

1 Introduction

Resveratrol is a phenolic compound classified as a stilbene derivative (with a C6-C2-C6 structure), which is found in plants such as red grape, peanut and some roots. Despite both the *cis* and *trans* molecular conformations of the compound can be found, the biological activity and increased stability is usually attributed to the trans-isomer (Burns, Yokota, Ashihara, Lean, & Crozier, 2002; Chedea et al., 2017). As many health benefits (e.g. antioxidant, anti-inflammatory and anticarcinogenic) have been associated to resveratrol (Rauf et al., 2017), its use as a nutraceutical in food, pharmaceutical and cosmetic products is quite desirable. However, its poor water solubility and chemical instability limit its use in the crystalline form.

Oil-in-water emulsions have been frequently used for resveratrol encapsulation because its solubility in oily matrices (~0.047–0.180 mg.mL^{-1} in vegetable oils - Hung, Chen, Liao, Lo, and Fang (2006)) is higher than in water (~0.03 mg.mL^{-1} -Amri, Chaumeil, Sfar, and Charrueau (2012)). Formulations have used many types of surfactants and stabilizing agents, like proteins (Duan et al., 2016; Hemar, Cheng, Oliver, Sanguansri, & Augustin, 2010; Matos, Gutierrez, Coca, & Pazos, 2014; Wan, Wang, Wang, Yang, & Yuan, 2013; Zhang, Khan, Cheng, & Liang, 2019), lecithin (Donsi, Sessa, Mediouni, Mgaidi, & Ferrari, 2011; Salgado, Rodríguez-Rojo, Alves-Santos, & Cocero, 2015; Sessa et al., 2014), starches and gums (Cardoso, Gonçalves, Estevinho, & Rocha, 2019; Matos et al., 2018), combination of these materials (Chen et al., 2020; Cheng et al., 2020; Feng, Yue, Wusigale, Ni, & Liang, 2018; Shao, Feng, Sun, & Ritzoulis, 2019) and others (Díaz-Ruiz et al., 2020; Matos, Gutiérrez, Iglesias, Coca, & Pazos, 2015). The use of Maillard-glycated protein-polysaccharide conjugates has been suggested as a promising alternative for use as stabilizing/emulsifying agents, because they can present improved functional properties in comparison to the proteins themselves. Enhanced emulsifying, foaming, stabilizing and solubility properties have been reported as some of the advantages of the use of Maillard reaction products for emulsification purposes (Bouyer, Mekhloufi, Rosilio, Grossiord, & Agnely, 2012; Li et al., 2019; Nooshkam, Varidi, & Verma, 2020; Oliver, Melton, & Stanley, 2006; Zha, Dong, Rao, & Chen, 2019). Furthermore, Maillard conjugates have also shown increased antioxidant capacity in comparison to non-reacted proteins (Consoli et al., 2018; Kchaou, Benbettaieb, Jridi, Nasri, & Debeaufort, 2019; Zhang et al., 2020), which can provide additional protection to the encapsulated bioactive compounds.

Traditionally, emulsification techniques employ mechanical devices like rotor-stator, high-pressure homogenizers/ microfluidizers or, more recently, sonication probes (Jafari, Assadpoor, He, & Bhandari, 2008b). Droplet disruption is the main mechanism of droplet formation in these methods, leading to broad polydispersity and demanding high energy consumption (Schubert & Engel, 2004; Silva, Cerqueira, & Vicente, 2012).

Membrane emulsification is a more recent technique though it has been already recognized for its capacity to enable the production of controlled-sized droplets with very low polydispersity. The droplets are formed when the disperse phase is forced into the continuous phase through the pores of a membrane, where they are usually detached by some shear applied over the membrane surface (Piacentini, Drioli, & Giorno, 2014; Spyropoulos, Lloyd, Hancocks, & Pawlik, 2014). Shear

needed for drop detachment is low compared to other emulsification methods therefore represents an alternative method regarding heat and shear sensitive compounds (Piacentini et al., 2014; Vladisavljević, 2019). Metallic membranes have some advantages like pores of very well defined size and increased chemical and mechanical resistance compared to other systems (Silva, Morelli, Dragosavac, Starov, & Holdich, 2017; Suárez, Gutiérrez, Coca, & Pazos, 2013). Furthermore, their use enables process employment for food-grade products.

To ensure products microbiological stability, avoid the risk of chemical and/or biological degradations, reduce the storage and transport costs, and finally obtain a product with specific properties like instantaneous solubility, conversion of the emulsion into dry powder is desired (Gharsallaoui, Roudaut, Chambin, Voilley, & Saurel, 2007). For this finality, spray drying is considered a reproducible, affordable, time-saving and scalable process (Salama, 2020).

The encapsulation process combining membrane emulsification and spray drying presents the advantage of controlled-sized droplets in the emulsions, which is important to ensure homogeneous distribution of the encapsulated material within the carrier agents, associated with the increased product stability of the powder reached by the water removal by the spray drying. Despite the many benefits provided by the integration of emulsification and spray drying processes, few studies have been performed regarding the membrane emulsification technique (Berendsen, Güell, & Ferrando, 2015; Choi et al., 2012; Mustapha et al., 2017; Oh et al., 2013, 2014; Ramakrishnan et al., 2013; Ramakrishnan, Ferrando, Aceña-Muñoz, De Lamo-Castellví, & Güell, 2013; Wang et al., 2020; Yang et al., 2013) and to the best of our knowledge, this association between both processes has not been carried out for resveratrol encapsulation.

The main purpose of our work was to combine membrane emulsification with the spray drying to encapsulate resveratrol, evaluating the effect of the process on the products properties. In this sense, the paper comprises a study for the definition of optimum emulsification process conditions, an evaluation of the phases' composition on emulsions properties and the study of the spray drying process in the microparticles resveratrol content and physicochemical properties.

2 Materials and methods

2.1 Materials

Sodium caseinate (NaCas) (90.7 g protein/100 g on dry weight basis, determined by Kjeldahl method, conversion factor 6.38) was a donation from Alibra Ingredients (Campinas, SP, Brazil). Maltodextrin MOR-REX 1910 (Dextrose Equivalent (DE) = 9–12) and Dried Glucose Syrup (DGS) MOR-REX 1930 (DE = 26–30) were supplied by Ingredion Brazil Industrial Ingredients Ltd. (Mogi-Guaçu, SP, Brazil). Refined palm oil (PO) was acquired from Naissance (Neith, UK). Resveratrol (98% purity), used in the formulations, was kindly donated by Naturex (São Paulo, SP, Brazil). Resveratrol HPLC grade (≥99% purity) and Nile Red dye were supplied by Sigma Aldrich Company Ltd. (Gillingham, Dorset, UK). All other materials were of analytical grade. Palm oil was chosen over other vegetable oils because of its high saturated fatty acids concentration (48%, according to Gunstone (2005)), which makes it more chemically stable and therefore could avoid excessive resveratrol oxidation within the system.

2.2 Emulsions preparation

For the continuous phase, NaCas, maltodextrin and DGS were dispersed individually in Milli-Q water containing 0.01% sodium azide. Each dispersion was stirred overnight at room temperature (~20 °C) using a magnetic stirrer. Then, the three dispersions were mixed giving a total solid concentration of 27 g/100 g with a 1/1/1 (NaCas/maltodextrin/DGS) ratio, and the pH was adjusted to 7.5 using NaOH 1 M. This first aqueous mixture will be further on referred to as "the non-heated mixture". The Maillard conjugates were prepared using a wet-heating method previously described by Consoli et al. (2018), with some modifications. Briefly, about 500 g of the non-heated mixture were transferred to a Schott Duran® bottle and sealed. The container was immersed in a water bath at 75 °C and kept for 6 h. After this period, the reaction was ceased by soaking the bottle in an ice bath. The pH was readjusted to 7.5 using NaOH 1 M.

The dispersed phase was mainly composed by PO. Nile Red dye was initially added to it to enable the visualization of the oil phase flowing into the non-heated mixture, which was quite opaque. When was the case, resveratrol was first solubilized in 99.5% ethanol (50 mg resveratrol/g ethanol), and this solution was mixed with PO for 1 min at 50 °C, using a magnetic stirrer. Emulsions had total solid concentration of 30 g/100 g for suitability to the spray drying process. Formulations used in each stage of the work are shown in Table 1. All the emulsification experiments, regarding process parameters and phase composition evaluation, were performed in duplicate.

Table 1

> (i) The table layout displayed in this section is not how it will appear in the final version. The representation below is solely purposed for providing corrections to the table. To preview the actual presentation of the table, please view the Proof.

Process parameters for membrane emulsification and spray drying process and emulsions composition in each stage of the work.

Set of experiments	1st stage	2nd stage	3rd stage
Objective	Definition of optimum process conditions	Study of the influence of the phases' composition	Spray drying of emulsions and powder characterization
Process Conditions	− Transmembrane flux of 35 and 70 L m^2 h^{-1} with shear stress of 0.4; 5.2; 16.6; 35.5 and 60.0 Pa;	− Shear stress 60.0 Pa and transmembrane flux of 70 L m^2 h^{-1}	*Emulsions:* shear stress 60.0 Pa and transmembrane flux 70 L m^2 h^{-1} *Spray drying:* Air inlet temperature: 180 °C; Air outlet temperature: 97 °C; emulsion feed rate: 10 mL.min^{-1}; Drying air flow rate: 30 m^3 h^{-1}; Compressed air flow rate: 2 m^3 h^{-1}; Compressed air operating pressure: 2 – 4 bar.

	– Shear stress constant at 60.0 Pa and transmembrane flux of 350; 500; 700 and 2000 L m^2 h^{-1}					
Continuous phase (95 g/100 g emulsion)	Non-heated mixture NaCas 8.9 g/100 g Maltodextrin 8.9 g/100 g DGS – 8.9 g/ 100 g emulsion	Maillard-reacted mixture (Heated at 65 °C for 6 h)				Maillard reacted mixture (Heated at 65 °C for 6 h)
Dispersed phase (5 g/ 100 g emulsion)	PO (5 g/ 100 g emulsion) + NRD (0.002 g/ 100 g oil)	PO (5 g/ 100 g emulsion) + NRD (0.002 g/100 g oil)	PO (5 g/100 g emulsion)	PO (4.6 g/ 100 g emulsion) + ethanol (0.40 g/ 100 g emulsion)	PO (4.5 g/100 g emulsion) + ethanol (0.40 g/ 100 g emulsion) + RSV (0.02 g/ 100 g emulsion)	PO (4.5 g/100 g emulsion) + ethanol (0.40 g/100 g emulsion) + resveratrol (0.02 g/100 g emulsion)

Abbreviations: PO – palm oil; NRD – Nile red dye; RSV: resveratrol.

A Dispersion Cell (Micropore Technologies, Wilton Centre, UK) was employed for emulsions preparation (Piacentini, Giorno, Dragosavac, Vladisavljević, & Holdich, 2013). In this equipment, the continuous phase is placed within a glass cylinder, into which the dispersed phase is pumped through a flat metal membrane placed at the bottom. Droplets are formed by the shear stress exerted by a paddle blade stirrer placed within the glass cylinder, right above the membrane. The stirrer is controlled by a DC power supply (Kenwood PA36-3A) where the user sets the voltage correspondent to the desired paddle rotation speed. The shear stress depends on the stirrer speed and on the continuous phase density and viscosity, and can be calculated using Eq. (1) (τ_{max} - maximum shear stress on the membrane surface) or Eq. (2) (τ_{av} - average shear stress on the membrane surface - Dragosavac, Sovilj, Kosvintsev, Holdich, and Vladisavljević (2008)).

$$\tau_{\max} = 0.825\eta\omega r_c \frac{1}{\delta}$$

(1)

$$\tau_{av} = \frac{6.6}{D_m^2}\eta\omega\frac{1}{\delta}\left\{\frac{r_c^3}{3} + \frac{r_c^{1.6}}{1.4}\left[\left(\frac{D_m}{2}\right)^{1.4} - r_c^{1.4}\right]\right\}$$

(2)

where D_m is the effective membrane diameter [m]; η is the continuous phase viscosity [Pa.s]; ω is the angular velocity [rad. s^{-1}]; δ is the boundary layer thickness [m], given by Eq. (3) (Landau & Lifshitz, 1959):

$$\delta = \sqrt{\frac{\eta}{\rho\omega}}$$

(3)

ρ is the continuous phase density [kg.m^{-3}];

And the critical radius r_c [m], which corresponds to the point where the rotation changes from a forced vortex to a free vortex, at which shear stress is greatest, is calculated using Eq. (4) (Nagata, 1975)

$$r_c = 1.23\frac{D}{2}\left(0.57 + 0.35\frac{D}{T}\right)\left(\frac{b}{T}\right)^{0.036}n_b^{0.116}\frac{Re}{1000 + 1.43Re}$$

(4)

where D is the stirrer diameter [m]; T is the tank (cell) diameter [m]; b is the blade height [m]; n_b is the number of impeller blades and Re is the Reynolds number, given by Eq. (5). Table 2 contains the values/dimensions used within the Eqs.

$$Re = \frac{\omega\rho D^2}{2\pi\eta}$$

(5)

Table 2

ⓘ The table layout displayed in this section is not how it will appear in the final version. The representation below is solely purposed for providing corrections to the table. To preview the actual presentation of the table, please view the Proof.

Membrane and formulation data used to perform the mathematical model calculations. This data refers to the formulations that had the non-heated mixture as continuous phase and the Nile red dye as the disperse phase, which was the one used in the first stage of the work.

Property	Symbol	Value
Equilibrium interfacial tension	σ_{eq}	7.06 mN.m^{-1}
Dispersed phase viscosity	η_{dp}	26.22 ± 0.08 mPa.s
Continuous phase viscosity	η_{cp}	108.40 ± 2.52 mPa.s
Continuous phase density	ρ_{cp}	1.11 kg.m^{-3}
Interpore distance	L	100 μm
Pore diameter	$\varnothing_p$	11.82 μm
Pore radius	r_p	5.86 μm
*Membrane effective diameter	$\varnothing_m$	3.40 cm
**Membrane effective surface area	S_m	9.08 cm^2
Tank cell diameter	T	4.00 cm
Stirrer diameter	D	3.00 cm
Blade height	b	1.10 cm
Number of blades	n_b	2 units

Table Footnotes

* The effective diameter considers the space taken by the gasket used to seal the tank cell.

** Surface area is based on membrane effective diameter.

Full nickel membranes of nominal pore size 10 μm, distributed in hexagonal array, interpore distance of 200 and 100 μm, effective membrane area of 9.08×10^{-4} m^2, and porosity (ε - Eq. (6)) of 0.0125 were used.

$$\varepsilon = \frac{\pi}{2\sqrt{3}}\left(\frac{d_p}{L}\right)^2$$

(6)

where d_p is the pore diameter and L is the interpore distance.

PO was kept at 52 °C to avoid crystallisation, using a jacketed syringe coupled to a thermostatic water bath. A syringe pump (WPI-World Precision Instruments Inc., AL-1000, UK) was used to inject it into the continuous phase, which was kept at 35 °C by placing the dispersion cell into a water bath.

Membrane cleaning was performed after each experiment by sonicating for 5 min, sequentially, the membrane immersed in soapy water, 4 M NaOH and 0.10 M citric acid. The membrane was additionally sonicated in distilled water after each of these solutions.

2.2.1 Droplet size prediction

A mathematical approach based on a force balance on the membrane pore (Kosvintsev, Gasparini, Holdich, Cumming, & Stillwell, 2005) was used for droplet size prediction. From Eq. (7), two models were fit to the data. Models I and II assume $\tau = \tau_{\text{average}}$ (Eq. (2)) and $\tau = \tau_{\text{maximum}}$ (Eq. (1)), respectively.

$$x = \frac{\sqrt{18\tau^2 r_p^2 + 2\sqrt{81\tau^4 r_p^4 + 4r_p^2\tau^2 Y^2}}}{3\tau}$$

(7)

where x is the predicted droplet diameter [m]; τ is the shear stress on the membrane surface [Pa]; r_p is the membrane pore radius [m] and Y is the interfacial tension [N m^{-1}] between the dispersed and continuous phases. Table 2 presents the main values used in the calculations.

Models do not consider the injection rate, which do have an effect on the final drop size (Schröder & Schubert, 1999). It predicts the 'smallest' theoretical drop size formed at the zero flux, where the finite time required to detach a droplet can be neglected. If drop formation time, t_d (s), is longer than that needed to inject a volume V_o, predicted by the simple force balance (Eq. (7)) then the volume of the droplet can be written as:

$$V = V_0 + t_d.J$$

(8)

where $t_d J$ is the extra volume of the drop caused by operating at a high injection rate J (L/s) during the finite time required for droplet formation (Matos, Suárez, Gutiérrez, Coca, & Pazos, 2013). However, in order to apply Eq. (9), the drop formation time must be assessed by the ratio of the volume of the droplet produced and the volume flowrate through a single pore of the membrane:

$$t_d = \frac{2\varepsilon k D_{(4,3)}^3}{3 d_p^2 J_d}$$

(9)

where ε is the porosity of the membrane (Eq. (6)), k is the percentage of active pores, $D_{[4,3]}$ is the volume-weighted mean droplet diameter (m) and d_p is the diameter of a pore (m). The fraction of pores that are actively generating drops is a rarely known value which usually has to be estimated (Morelli, Holdich, & Dragosavac, 2017). Thus, for illustrating the key parameters influencing the drop formation in the system studied in this work, only the simple force balance model (Eq. (7)) is compared to the experimental data (Fig. 2) and any calculations of drop formation time will use the estimate of 50% pore utilisation. Results calculated for our system are summarized in Table 3. The readers are very welcome to check detailed information about the calculations in the Supplementary Material.

Table 3

ⓘ The table layout displayed in this section is not how it will appear in the final version. The representation below is solely purposed for providing corrections to the table. To preview the actual presentation of the table, please view the Proof.

Stirrer speed employed in the Dispersion Cell in the membrane emulsification process, in the first stage of the work, with their correspondent maximum shear stress (Eq. (1)) and average shear stress (Eq. (2)). The estimate droplet formation time (Eq. (9)) was calculated for each stirrer speed and dispersed phase flux employed during the study of the influence of process conditions on emulsions properties (first stage of the work). Emulsions composition: non-heated mixture as continuous phase (95 g/100 g emulsion); palm oil and Nile red dye as dispersed phase (5 g/100 g emulsion).

Stirrer speed (rpm)	Max. shear stress (Pa)	Average shear stress (Pa)	Feed rate (mL min^{-1}) / Dispersed phase flux J_d (L h^{-1} m^{-2})					
			0.5/ 35	1.0/ 70	5.0/ 350	7.5/ 500	10.0/ 700	30.0/ 2000
			Droplet formation time (s)					
200	0.4	0.1	2.501 ± 0.633 [aB]	1.687 ± 0.566 [aB]				
575	5.2	1.5	1.112 ± 0.574 [aAB]	0.814 ± 0.039 [aAB]				
950	16.6	6.2	0.631 ± 0.063 [bA]	0.257 ± 0.058 [aA]				
1300	35.5	15.4	0.217 ± 0.021 [bA]	0.100 ± 0.015 [aA]				
1650	60.0	28.6	0.076 ± 0.007 [aA]	0.061 ± 0.007 [aA]	0.021 ± 0.002 [a]	0.013 ± 0.002 [a]	0.010 ± 0.004 [a]	0.008 ± 0.000 [a]

Values are averages of two experiments, with each individual sample analysed in triplicate regarding droplet size, which is considered to droplet formation time calculation. Different lowercase letters in the same row represent statistically significant difference ($p \le 0.05$). Different capital letters in the same column represent statistically significant difference ($p \le 0.05$).

2.3 Emulsions characterization

To determine the interfacial tension between the oil and water phases of the emulsion, a tensiometer Tracker-S (Teclis, Longessaigne, France) was used employing the pendant droplet method. The initial volume was 7 μL, and measurements were taken until the equilibrium between the phases was reached. Analyses were performed at 50 °C to ensure complete melting of PO.

Emulsions droplet size was evaluated using a laser diffraction system Mastersizer 2000 (Malvern Instruments Ltd., Malvern, UK). Mean droplet diameter was expressed as D_{50}, which represents the diameter of cumulative distribution of 50% of total droplets. Polydispersity of droplet size was determined as the *Span = $(D_{90} - D_{10})/D_{50}$*, where D_{10}, D_{50}, and D_{90} represent the diameter of cumulative distribution of 10%, 50% and 90% of total droplets, respectively.

To confirm data obtained using Mastersizer 2000, a small droplet of each emulsion was placed on a slide and the sample was observed using an optical microscope GT Vision FXM-L3201(GT Vision Ltd., Stansfield, UK) coupled to a QImaging digital camera (QImaging Ltd, Surrey, Canada), with 100× or 200× magnification. Images were captured using the QCapture Suite 2.98.2 software.

2.4 Spray drying of emulsions

Resveratrol-loaded emulsions were spray-dried using a lab scale SD06 Spray Dryer (Labplant UK Ltd, Hunmanby, UK). Emulsions were fed into a two-fluid atomizer with a nozzle diameter of 0.5 mm, using the peristaltic pump coupled to the equipment. Table 1 lists all the parameters used in this process. The process parameters were based in a previous work of our research group, in which the same carrier materials were employed (Consoli, Dias, da Silva Carvalho, da Silva, & Hubinger, 2019). The yielded dried powder was collected from the cyclone and the recovery chamber and was stored in airtight containers. Experiments were performed in duplicates.

2.4.1 Powder characterization

To obtain moisture content of powder, samples were kept in a drying oven at 105 °C until reaching constant mass (AOAC, 2005). For particle size measurement, the powder was dispersed in 99.5% ethanol and analysed using laser diffraction system Mastersizer 2000 (Malvern Instruments Ltd., Malvern, UK). The volume-weighted diameter $D_{[4,3]} = \Sigma n_i D_i^4 / (\Sigma n_i D_i^3)$ was used to represent the mean particle size, where n_i is the number of droplets with diameter D_i. Span was used to express particle polydispersity.

Particles microstructure was observed using Scanning Electron Microscopy (SEM). Spray-dried powder was placed over carbon tapes and fixed on the surface of stubs. A Q150-T Turbo-Pumped Sputter Coater (Quorum Technologies, Laughton, East Sussex, UK) was used to cover the particles with a metal layer formed by

80% Gold and 20% Palladium. The stubs were observed using a Tabletop Scanning Electron Microscope (SEM) TM3030 (Hitach High-Technologies Corporation, Krefeld, Germany), with an energy dispersive X-ray detector. Images were captured at 1000× and 3000× magnification.

Emulsion reconstitution analysis was performed as described by Drapala, Auty, Mulvihill, and O'Mahony (2017) with some modifications. 5 mL of distilled water were added to 0.6 g of powder. The mixture was stirred manually until complete dissolution. Sample was characterized by means of droplet size and optical microscopy, as previously described (Section 2.3).

2.4.2 Resveratrol quantification

Sample preparation followed the method by Consoli et al. (2019), with some modifications. To obtain resveratrol total content, 0.25 g of powder was placed in a plastic tube with 2.5 mL of milli-Q water. Sample was stirred manually for 1 min, and 7.5 mL of acetonitrile was added to the mixture, followed by manual stirring for 1 min. The tubes were centrifuged at 3,500 rpm for 15 min using a Heraeus Labofuge 400 Centrifuge (Thermo Fisher Scientific, Winsford, UK), at room temperature (~20 °C). The supernatant was collected and placed apart. 2.5 mL of milli-Q water was added to the precipitate and the process was repeated until centrifugation. The supernatant was collected and mixed with the supernatant fraction from the first centrifugation. Two drops of formic acid were added to this mixture followed by centrifugation for 35 min at 3500 rpm. To determine resveratrol superficial content, 0.5 g of powder were placed within a plastic tube with 5 mL of 99.5% ethanol. Each tube was inverted manually for 5 min followed by gravitational filtration through filter paper Whatman® (CAT No 2200 150; GE Healthcare Life Sciences, Little Chalfont, UK). Samples prepared both ways were filtered through polyethersulfone (PES) syringe filters 0.22 μm (Millex®GP Millipore Express, Merck Millipore Ltd, Tullagreen, Ireland) into glass vials and frozen until HPLC analysis.

HPLC analyses were performed using an Agilent 1100 series (Agilent Technologies, Santa Clara, USA) liquid chromatograph equipped with a diode array detector (DAD G1315B), a degasser (G1322A), a quaternary gradient pump (G1311A), an autosampler (ALS G1313A) and a column oven (Colcom G1316A). 10 μL of sample, prepared as just described, was injected in a reversed phase C_{18} column (Kinetex 5 μm, 100 × 4.60 mm, Phenomenex, Macclesfield, UK) kept at 25 °C. The solvents (solvent A = milliQ water:formic acid 99.8:0.2; solvent B 100% acetonitrile) and flow rate (0.8 mL.min^{-1}) were based on a previous work (Ji, Li, Ji, & Lou, 2014). The linear solvent gradient ran as follows: 0 – 2 min: 60% A and 40% B; 5 min: 42% A and 58% B; 7 min: 60% A and 40% B. The UV detector was set to monitor the wavelength at 306 nm. Standard solutions of concentration ranging from 3 to 15 mg.L^{-1} were evaluated along with the samples and were used to determine the concentration of resveratrol in the samples.

2.4.3 Process efficiency and encapsulation efficiency

The ratio at which total resveratrol (RSV) added to the formulation was retained in the spray-dried particles was defined as the process efficiency (PE) and was calculated from Eq. (10).

$$PE[\%] = \frac{total\ RSV_{HPLC}}{total\ RSV_{weighed}} \times 100$$

(10)

Encapsulation efficiency (EE) was defined as the ratio between the actual amount of resveratrol entrapped *within* the particle (not on its surface), and the total amount of resveratrol determined by HPLC (Eq. (11)).

$$EE[\%] = \frac{(total\ RSV_{HPLC} - superficial\ RSV_{HPLC})}{total\ RSV_{HPLC}} \times 100$$

(11)

Results were statistically analysed by Tukey test, where differences between means were considered at a 5% significance level (p ≤ 0.05). Microsoft Excel (2016 version) was employed to perform the statistical analyses, using the "Data Analysis" tool.

3 Results and discussion

3.1 The influence of process parameters on emulsions properties

Droplet size is an important emulsion property as it is related to the emulsion kinetic stability, viscosity and to the encapsulation efficiency of bioactive compounds when emulsions are used as vehicles for specific compounds (Jafari, Assadpoor, He, & Bhandari, 2008a; McClements, 2005).

In membrane emulsification, the shear stress over the membrane surface is one of the main factors to affect droplet diameter, since it is directly related to droplet detachment from the membrane surface. It should be provided within a range that is sufficient to promote the required tangential shear on the membrane surface, yet not too high to cause droplet disruption after production (Vladisavljević & Williams, 2005).

Initially, emulsions were prepared using the same formulation employed for resveratrol encapsulation in our previous works (Consoli et al., 2019, 2017, 2018), where emulsions had 30 g/100 g solid concentration with a lower NaCas/maltodextrin/DGS ratio (1/2.5/2.5). Even though mean droplet size was not much big (~55 μm), emulsions had poor kinetic stability due to the relatively low viscosity of the continuous phase (17.4 mPa.s), hence not suitable for spray drying. As an attempt to overcome this situation, we increased the NaCas/maltodextrin/DGS ratio to 1/1/1, which resulted in a much more viscous continuous phase (108.4 mPa.s) and no phase separation, enabling the spray drying process. This improved formulation was used during this entire work (Table 1), and the shear stress was varied only by changing the stirrer speed. Fig. 1 compares the microstructure of emulsions with different NaCas/maltodextrin/DGS ratios. Table 3 relates the shear stress obtained for each stirrer speed employed.
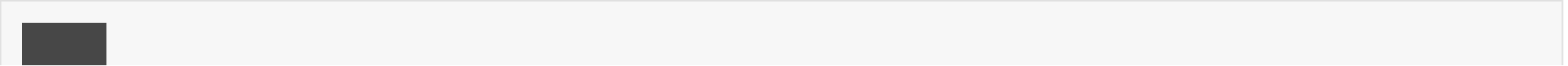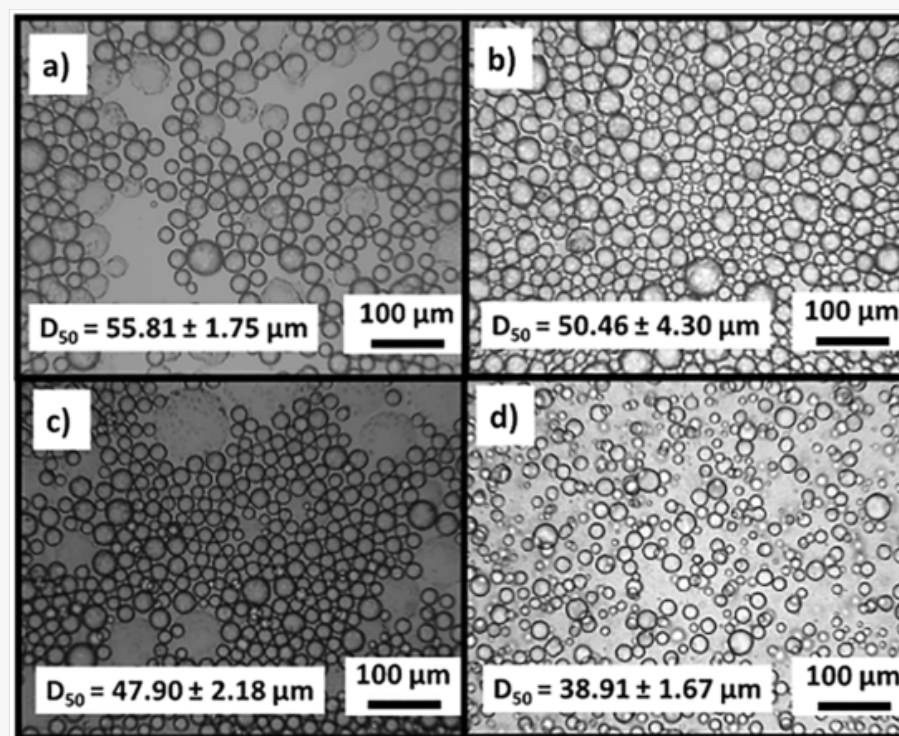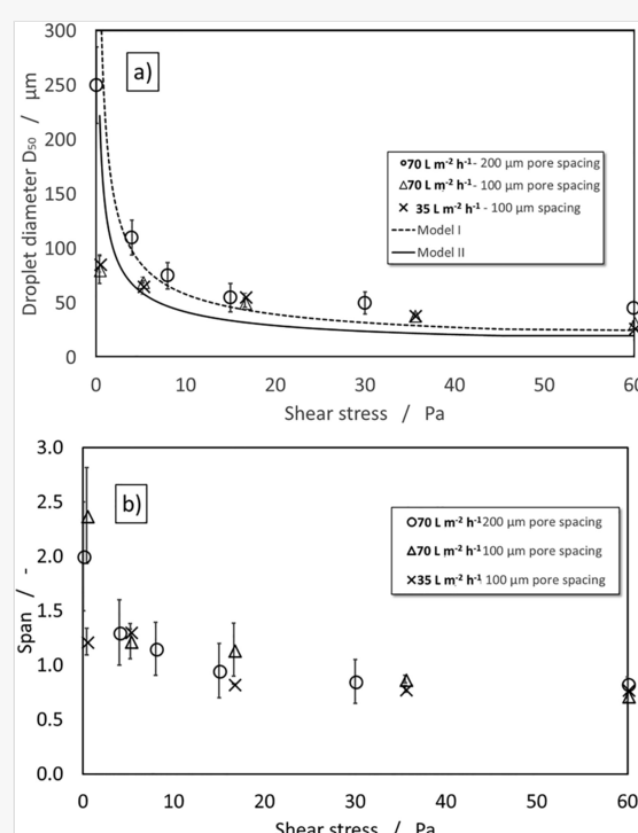
Micrographs of emulsions produced using different maximum shear stress and sodium caseinate/maltodextrin/DGS ratio. (a) 16.6 Pa and 1/2.5/2.5 ratio; (b) 16.6 Pa and 1/1/1 ratio; (c) 35.5 Pa and 1/2.5/2.5; (d) 35.5 Pa and 1/1/1 ratio. DGS: Dried Glucose Syrup.
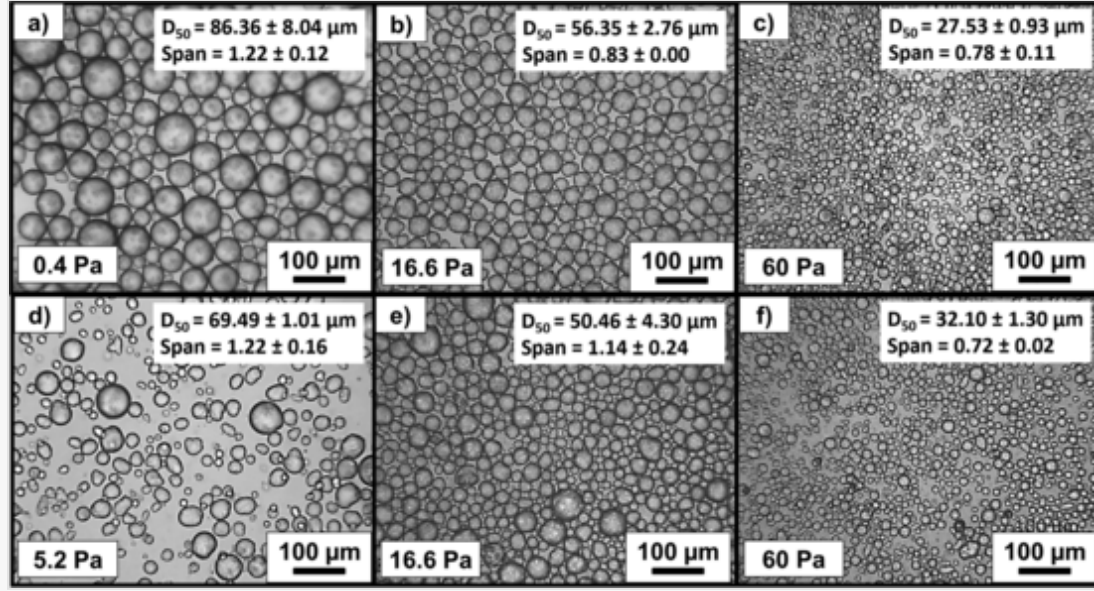
Emulsions droplet mean diameter (D_{50}) and Span, as a function of shear stress over the membrane surface, are shown in Fig. 2. Initially the membrane with 10 μm pore size and 200 μm pore spacing was used. Increase of rotation speed, and consequently shear stress, resulted in emulsions with smaller droplets and tighter size distribution (Fig. 2b). Droplets between 250 and 45 μm were produced with spans between 2 and 0.78 respectively (Fig. 2a-b). This behavior is in accordance to what has been reported in works that used a similar dispersion cell for membrane emulsification (Dragosavac et al., 2008; Imbrogno et al., 2015; Kosvintsev et al., 2005; Morelli et al., 2017; Piacentini et al., 2013; Stillwell, Holdich, Kosvintsev, Gasparini, & Cumming, 2007). According to Dragosavac et al. (2008), the reduction in droplet size over increased shear stresses occurs because of an increase in the drag force that acts on the droplets. In attempt to produce smaller droplet size with even tighter size distribution, membrane with 100 μm pore spacing was used to generate the emulsions. Dispersed phase fluxes of 70 and 35 L m^{-2}h^{-1} were used and smallest D_{50} produced was 27 μm with shear stress of 60 Pa. Although small difference could be detected in the size parameters of emulsions obtained at fluxes of 70 and 35 L m^{-2}h^{-1}, the values were statistically similar (p < 0.05). After the rotation speed was increased to higher than about 950 rpm (τ_{max} = 16.6 Pa), the difference in size became lower, apparently reaching a plateau. Indeed, statistical analysis showed similar results for D_{50} and Span when a minimum rotation speed of 950 rpm was applied over the membrane surface. Micrographs (Figs. 3 and 5) show visible difference in droplet diameter and size distributions under different conditions of shear and dispersed phase flux and they highlight the trend of decreased D_{50} and polydispersity at higher shear stresses applied on the membrane surface.

(a) Comparison between the theoretical droplet size calculated using Eq. (7), where model I assumes τ = τaverage (Eq. (2)) and model II assumes τ = τmaximum (Eq. (1)), and the experimental mean diameter D50 obtained under different conditions of shear stress for transmembrane fluxes and membrane pore spacing (100 and 200 μm). (b) Span of a droplet size distribution obtained under different conditions of shear stress for different fluxes and membrane pore spacing (100 and 200 μm). Emulsions composition: non-heated mixture as continuous phase (95 g/ 100 g emulsion); palm oil and Nile red dye as dispersed phase (5 g/ 100 g emulsion). Membrane pore size = 10 μm.
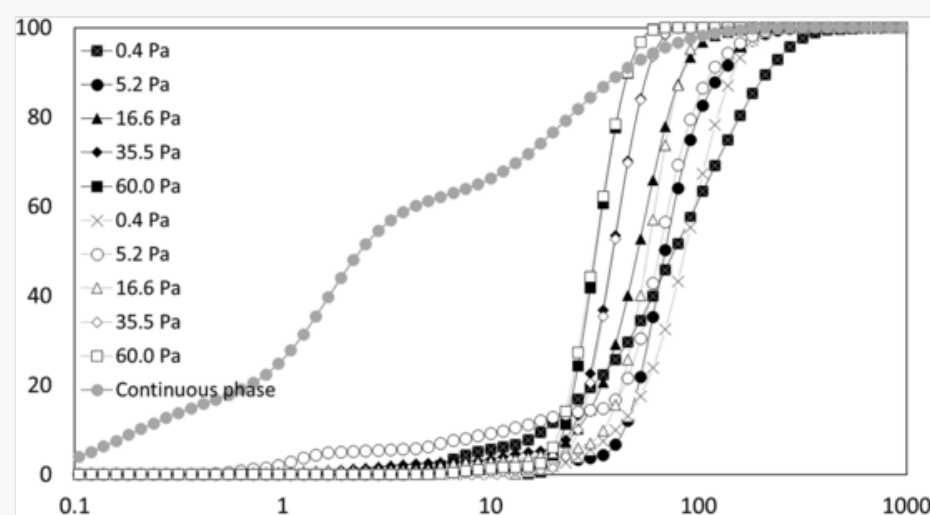
Images a), b) and c) illustrate micrographs of emulsions produced with transmembrane flux 35 L m^{-2}h^{-1}, whereas those in images d), e) and f) were produced using transmembrane flux 70 L m^{-2}h^{-1}. Emulsions composition: non-heated mixture as continuous phase (95 g/ 100 g emulsion); palm oil and Nile red dye as dispersed phase (5 g/ 100 g emulsion). Membrane pore size = 10 μm; membrane pore spacing = 100 μm.

Mathematical modelling has been frequently applied for droplet size prediction in membrane emulsification systems (Dragosavac et al., 2008; Dragosavac, Holdich, Vladisavljević, & Sovilj, 2012; Dragosavac, Vladisavljević, Holdich, & Stillwell, 2012; Imbrogno et al., 2015; Kosvintsev et al., 2005; Morelli et al., 2017; Santos, Vladisavljević, Holdich, Dragosavac, & Muñoz, 2015; Stillwell et al., 2007; Vladisavljević, Wang, Dragosavac, & Holdich, 2014). In Fig. 2a, models I and II (Section 2.2.1) were plotted against the experimental data. Models described by Eqs. (1), (2) and (7) do not consider the dispersed phase flux, therefore the model can be regarded as an indication of the smallest drop size that can be produced at the lowest injection flux. Combining Eqs. (8 and 9) together with the known injection flux and assuming membrane pore utilisation of 50%, it is possible to determine the droplet formation time t_d (Eq. (9)). As shows Table 3, it decreases from 1.69 s when operating at 0.4 Pa shear stress (200 rpm stirrer speed) to 0.06 s at 60 Pa (1,650 rpm). A significantly lower t_d with respect to shear (stirrer speed) appears to be a sensible result as it is consistent with drop size decrease when the shear is increased.

The effect of the shear stress on the droplet polydispersity can also be observed from Fig. 4. As shear stress was increased, the curves were shifted to the left and presented a steeper slope, indicating a narrower size polydispersity. The increase of transmembrane flux within the range from 35 to 70 L m^{-2}h^{-1} did not affect droplet size at constant shear stress, as evidenced by the curves overlaying.
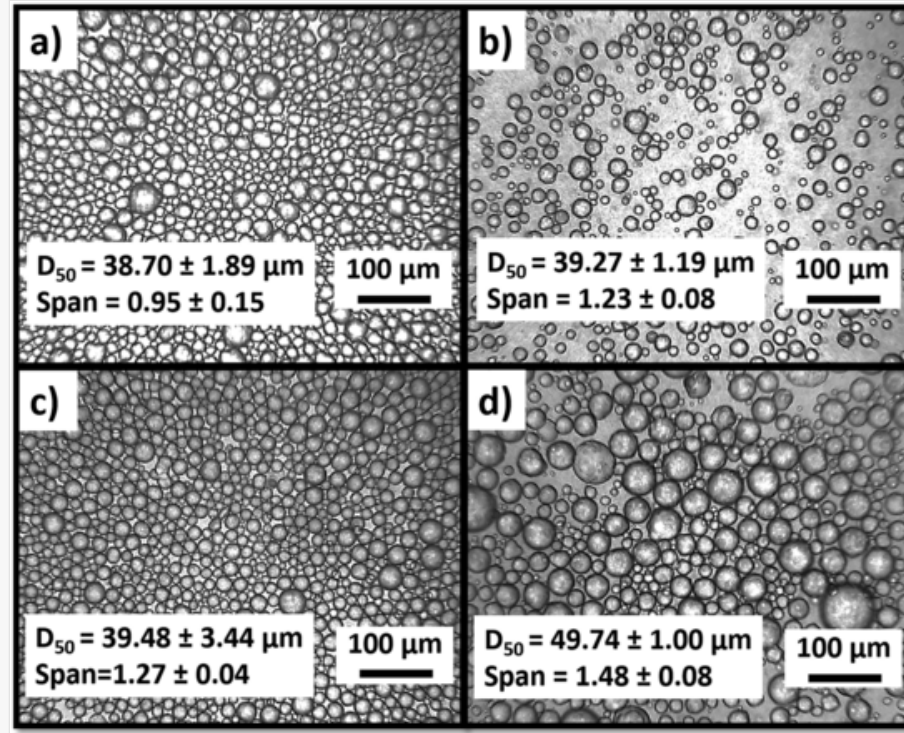
Fig. 4

(a) Particle size distribution at different shear stresses. Hollow symbols: dispersed phase flux = 35 Lm^{-2}h^{-1}; full symbols: dispersed phase flux = 70 L m^{-2}h^{-1}. Emulsions composition: non-heated mixture as continuous phase (95 g/ 100 g emulsion); palm oil and Nile red dye as dispersed phase (5 g/ 100 g emulsion). Membrane pore size = 10 μm; membrane pore spacing = 100 μm.

To investigate the effect of higher dispersed phase fluxes on the size parameters, we increased the flux to 2000 L m^{-2}h^{-1}, keeping shear stress of 60 Pa. Fig. 5 shows the micrographs of the emulsions produced under different transmembrane fluxes. At higher fluxes, t_d was quite fast, and droplets were bigger. It probably occurred because the protein molecules, which adsorb slowly over the droplets surface due to their high molecular mass (20–25 kDa for α-, β- and κ-casein, the main constituents of NaCas - Morris, Sims, Robertson, and Furneaux (2004)), could not cover the entire oil/water interface. Another factor that probably influenced for this result is that when most of the pores are active, droplets diameter is limited by the interpore distance (Dragosavac et al., 2008), because the adjacent droplets hinder each other to grow bigger than it. Indeed, the interpore distance of the membranes used in our work was 100 and 200 μm, and the highest mean diameter obtained were very close to these values. It is possible that at higher dispersed phase fluxes more pores were active which in combination with production of larger drops provided greater chance for droplets coalescence as similarly observed by Charcosset (2009).
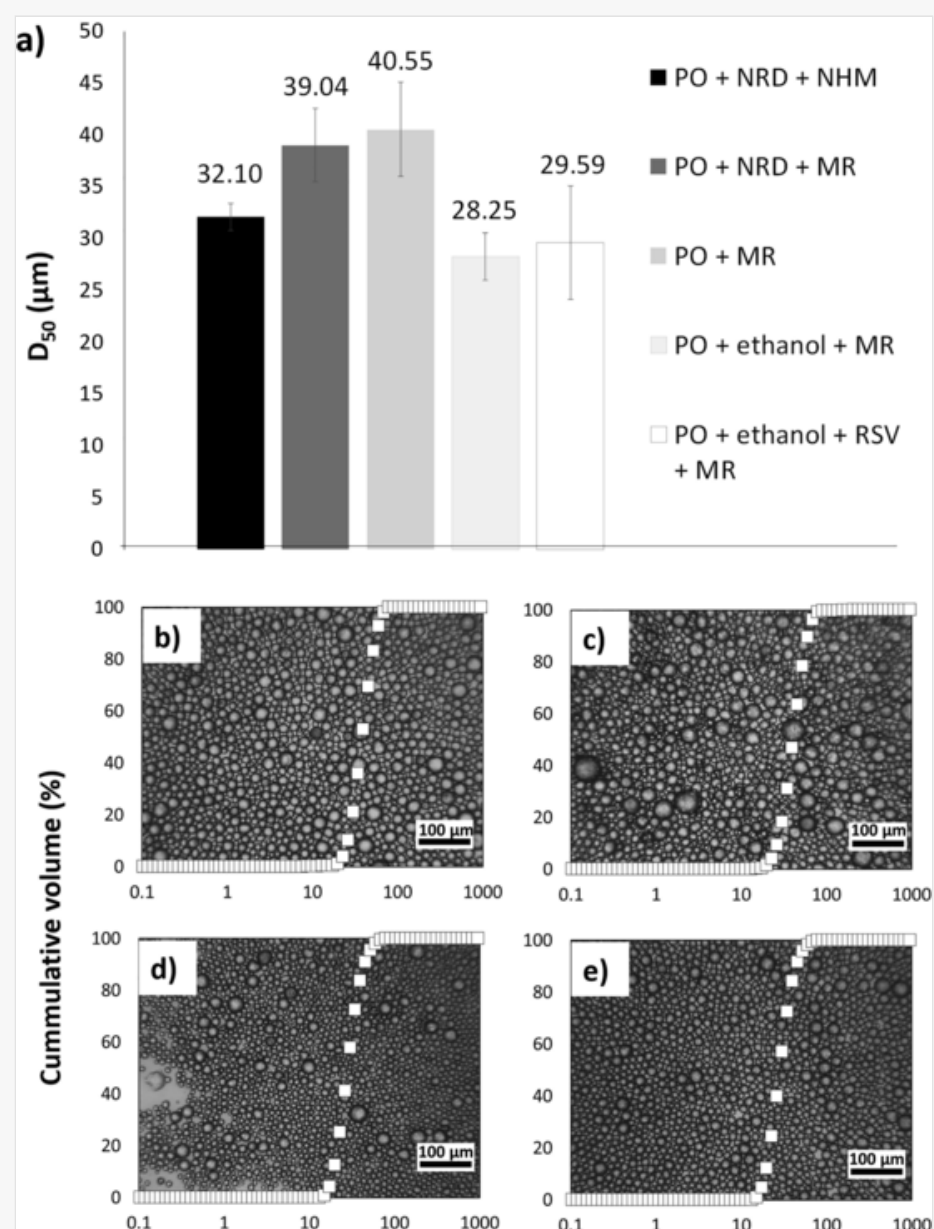
Fig. 5

Micrographs of emulsions produced using different transmembrane flux: (a) 350 (b) 500 (c) 700 and (d) 2000 L $m^{-2}h^{-1}$. Emulsions composition: non-heated mixture as continuous phase (95 g/ 100 g emulsion); palm oil and Nile red dye as dispersed phase (5 g/ 100 g emulsion). Membrane pore size = 10 μm; membrane pore spacing = 100 μm; shear stress = 60 Pa. (For interpretation of the references to colour in this figure legend, the reader is referred to the web version of this article.)

As our aim was to spray dry the emulsion, we set as conditions for continuity of the work the highest rotation shear stress (1650 rpm ~ τ_{max} = 60.0 Pa), since it provided the smallest droplet size with potentially lower probability to be broken within the spray dryer nozzle; and transmembrane flux of 70 L $m^{-2}h^{-1}$, because emulsions obtained in this conditions had mean droplet diameter significantly smaller than those produced at 350 L $m^{-2}h^{-1}$, and were as monodisperse as those obtained at 35.0 L $m^{-2}h^{-1}$.

3.2 The effect of continuous and dispersed phase composition

In this stage, we checked the effect of emulsion composition in the size parameters using four formulations other than the one used in the first stage (non-heated mixture + PO + Nile red dye) (Table 1). Mean diameter D_{50} is shown in Fig. 6a. Droplet size distribution of the emulsions is presented in Fig. 6b-e combined to the micrographs. More polydisperse emulsions with bigger droplets were obtained when Maillard-reacted continuous phase was employed without the addition of ethanol. Droplets were very uniform once ethanol was added, regardless of the presence of resveratrol.
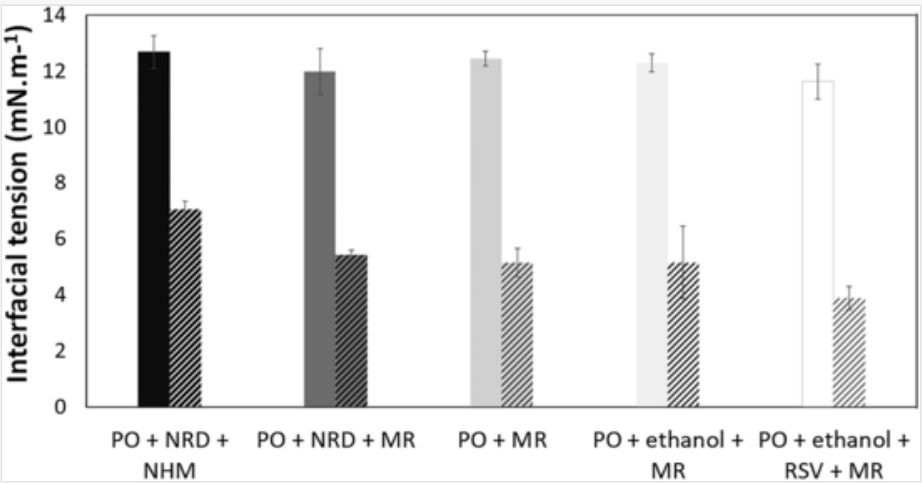
Fig. 6

The measurements of initial interfacial tension (Fig. 7) were virtually the same for all the formulations. A possible explanation is that the surface activity of NaCas, a protein with high emulsifying ability, must have dominated over the other components in the initial contact between the phases. Even though this protein is supposed to have undergone some structural modification in the Maillard-reacted samples, there were probably some remaining unreacted protein in the medium, which seems to have dominated in this initial stage of the measurement. The hydrolyzed starches used in the formulation have poor emulsifying ability (Reineccius, 2004) and have probably not exerted superficial activity. On the other hand, the equilibrium interfacial tension was more dependent on the composition: a substantial decrease was observed once the non-heated mixture was replaced by the Maillard-reacted continuous phase. The Maillard reaction is known for its ability to improve protein functional properties (Bouyer et al., 2012; de Oliveira, Coimbra, de Oliveira, Zuñiga, & Rojas, 2016; Oliver et al., 2006). Glycation of carbohydrates to NaCas molecules usually increase their solubility (O'Regan & Mulvihill, 2009; Shepherd, Robertson, & Ofman, 2000), which might have contributed for increasing diffusivity of the molecules and, consequently, better adsorption on droplet surface, thus reducing the interfacial tension in the o/w interface. Despite the reduction on the equilibrium interfacial tension, D_{50} and size distribution were larger in emulsions stabilized by the Maillard-reacted continuous phase, which probably happened because although the droplets surface had probably more protein molecules adsorbed, these molecules had undergone conformational change due to carbohydrates attachment through covalent bonds. Such attachment contributes to an increase on the protein 'hairy layer' over the oil droplet surface, which might have affected the laser measurements due to increase on the hydrodynamic diameter. Removal of Nile red dye from the oil phase did not affect D_{50} and equilibrium interfacial tension, showing that this chemical had no superficial activity in this system.

Fig. 7

Interfacial tension measurements obtained for the same combinations of continuous/ dispersed phases. Full color bars represent initial interfacial tension, whereas dashed lined bars represent the equilibrium interfacial tension for each system. Different lowercase letters indicate statistically significant difference at p < .05 in the same parameter (initial or equilibrium interfacial tension), between samples of different compositions. Different capital letters indicate statistically significant difference at p < .05 between initial and equilibrium interfacial tension, in samples of the same composition. Abbreviations: PO – palm oil; NRD – Nile red dye; NHM – non-heated mixture; MR – Maillard reaction continuous phase; RSV – resveratrol.

The equilibrium interfacial tension obtained in the presence of ethanol was virtually the same without it. However, the higher deviation over this measurement is an indicator that the equilibrium interfacial tension could be actually lower. The high temperature used in the analysis (50 °C), to avoid PO crystallization, can have influenced for the evaporation of the free ethanol in the system, thus causing this higher deviation. Ethanol has been reported to present co-surfactant activity in emulsions (J. L. Feng, Wang, Zhang, Wang, & Liu, 2009), suggesting that the equilibrium interfacial tension could have been reduced by the addition of this component, which corroborates to smaller D_{50} in emulsions with ethanol. Resveratrol addition to the oil phase caused no significant effect in the equilibrium interfacial tension and D_{50}. Since ethanol was bonded to resveratrol molecules for solvation, the effects of temperature on this measurement was not as strong as in the previous one. The low concentration of resveratrol (0.02 g/100 g emulsion) can have contributed for these results.

These findings highlighted the importance of emulsions phases composition for membrane emulsification. We also found that it would be possible to produce monodisperse emulsions with D_{50} as small as those in the emulsions of the first stage of the work, even after the use of the Maillard reacted mixture and the addition of ethanol and resveratrol.

3.3 Microparticles obtained by spray drying of membrane emulsification products

In this final stage of the work, resveratrol-loaded emulsions were spray dried to form fine microparticles.

The water content of spray-dried powders is a result from the combination of factors such as drying air inlet temperature, droplet residence time within the drying chamber, infeed liquid viscosity and solids concentration. As shows Table 4, microparticles total water content was about 3.6%, which is in accordance with results from previous works that employed NaCas as the main carrier material (Hogan, McNamee, O'Riordan, & O'Sullivan, 2001a, 2001b).

Table 4

ⓘ The table layout displayed in this section is not how it will appear in the final version. The representation below is solely purposed for providing corrections to the table. To preview the actual presentation of the table, please view the Proof.

Physico-chemical characterization of spray-dried particles. Particle size parameters are compared to those of the original emulsion (the one fed into the spray dryer) and the reconstituted emulsion (spray-dried particles solubilized with water). Emulsions composition: Maillard reacted mixture as continuous phase (95 g/100 g emulsion); palm oil, ethanol and resveratrol as dispersed phase (5 g/100 g emulsion).

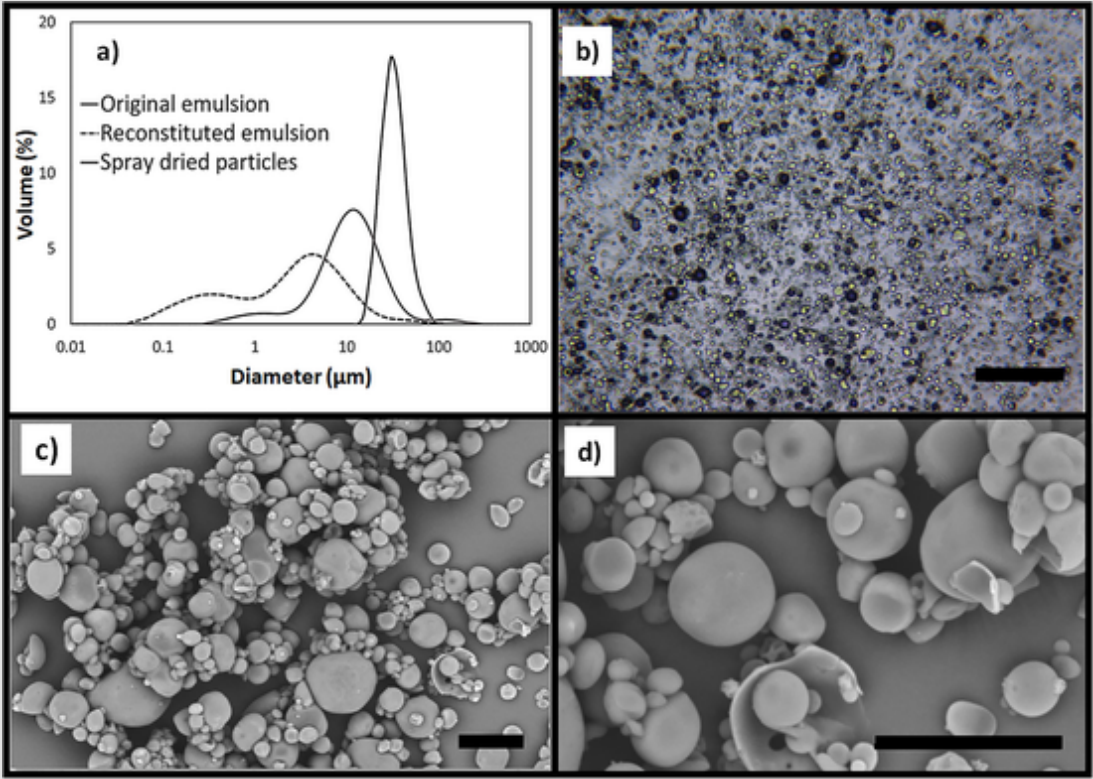| Sample	$D_{[4,3]}$ (µm)	$d_{(0.1)}$ (µm)	$d_{(0.5)}$ (µm)	$d_{(0.9)}$ (µm)	Span (dimensionless)	Water content (%)	Process efficiency (%)	Encapsulation efficiency (%)	Resveratrol loading (mg RSV/g powder)
Spray-dried particles	14.31 ± 1.11^a	2.98 ± 0.02^a	10.16 ± 0.46^a	25.35 ± 2.10^a	2.20 ± 0.10^a	3.58 ± 0.31	119.55 ± 0.75	97.71 ± 0.01	0.797 ± 0.004
Original emulsion*	31.49 ± 5.32^b	21.23 ± 4.13^b	29.59 ± 5.49^b	43.60 ± 6.98^b	0.76 ± 0.05^a	–	–	–	–
Reconstituted emulsion	4.52 ± 0.36^a	0.20 ± 0.01^a	2.54 ± 0.24^a	11.44 ± 1.57^a	4.18 ± 0.66^b				

Values are averages of two experiments, with each individual sample analysed in triplicate regarding each parameter. Different lowercase letters in the same column represent statistically significant difference (p ≤ 0.05).

Table Footnotes

[*] Original emulsion – Continuous phase: Maillard reacted compounds; Dispersed phase: Palm oil/Ethanol/Resveratrol. Shear stress = 60.0 Pa, Dispersed phase flux = 70 L h^{-1} m^{-2}. Reconstituted emulsions were prepared as described in Section 2.4.1.

Regarding microparticles size parameters (Table 4), mean diameter was around 10 µm (D_{50}) and 14 µm ($D_{[4,3]}$), which is convenient for application in food products without affecting mouthfeel attributes, as 30 µm is usually an acceptable limit for this condition (Herrera, Falabella, Melgarejo, & Añón, 1998). Polydispersity was relatively broad as evidenced by the curve in Fig. 8a and Span (~2.2).

Fig. 8

(A) Size distribution diagram comparing the original and the reconstituted emulsions to the spray-dried particles. (B) Micrograph obtained for the reconstituted emulsions at 200× magnification. Scale bar: 100 µm; and scanning electron microscopy (SEM) micrographs obtained for the spray-dried particles at (C) 1000× and (D) 3000× magnification. Scale bar: 25 µm.

In Fig. 8c-d microparticles present mostly smooth surface and spherical shape. The low molecular mass sugars present in DGS have probably exerted a plasticizing effect, avoiding shrinkage during the drying process hence corroborating to these surface characteristics (Takeungwongtrakul, Benjakul, & H-kittikun, 2015), which was reported in other works that employed DGS in spray-dried formulations (da Silva Carvalho et al., 2016; Drusch, Serfert, Scampicchio, Schmidt-Hansberg, & Schwarz, 2007; O'Dwyer, O'Beirne, Eidhin, & O'Kennedy, 2013). These characteristics contribute for a free-flowing powder, that is a very important feature regarding its application and packing. Micrographs in Fig. 8c-d also show samples polydispersity, where the smaller particles are mainly attached to the surface of the bigger ones, resulting in particle agglomeration. During drying, particles surface can become sticky due to the plastic behaviour of the low molecular mass sugars of DGS, which eases their adhesion and consequent agglomeration (Bhandari, Datta, & Howes, 1997).

Because of the situations in which particles are added to water-based products, emulsions reconstitution should be evaluated. Fig. 8a compares the size distribution diagrams of the original emulsion, which was fed into the spray dryer, the spray-dried particles and the reconstituted emulsions. Fig. 8b presents the micrograph of the reconstituted emulsion. The spray-dried particles had smaller mean droplet diameter compared to the original emulsions. The reconstituted emulsions presented even smaller mean diameter (Table 4), with a much broader size distribution. Two-fluid atomisers, like the one in the spray dryer used in our work, operate with high atomization pressure in the nozzle (from 2 to 4 bar in our system), which is intended to break down the infeed liquid into very small drops, increasing the surface area for heat and mass exchanging with the inlet air for higher drying efficiency (Gharsallaoui et al., 2007). In our system, the high pressure in the nozzle is the most likely reason for the decreased droplet size of the reconstituted emulsions, and also for the size of the solid microparticles formed, since they are smaller than the infeed emulsion droplets themselves.

Determining the process efficiency is important to quantify possible losses of the encapsulated compound during the process. The combination of membrane emulsification to spray drying did not cause resveratrol losses, since process efficiency was 119.55%. This value higher than 100% was probably obtained because the high temperature of the inlet air can have caused the evaporation of other components in the formulation, such as the ethanol used to solubilize resveratrol, and made the final product even drier than the original materials used in the emulsions (NaCas, maltodextrin and DGS), by removing their intrinsic water. Another possibility, presented by Maschke et al. (2007) for a similar situation, is that part of the carrier material might have been lost within the nozzle.

In studies concerning the effects of resveratrol on human health, resveratrol daily intake ranges from 10 mg to 2 g (Lam, Peterson, & Ravussin, 2013), even though the safety limit is taken as 1 g/day (Patel et al., 2011). Red wine is one of the most known dietary sources of resveratrol, with concentration ranging from 0.1 to 14.3 mg.L^{-1} (Brown et al., 2009). Moderate consumption of red wine (100 mL/day for women and 200 mL/day for men) is associated to beneficial effects regarding cardiovascular diseases and great part of it is attributed to resveratrol bioactivity (Artero, Artero, Tarín, & Cano, 2018). In this sense, 1 g of the spray-dried powder produced in our work would be able to replace about 100 mL of red wine (~one glass) and could then be used as vehicle for this compound to be added in food/pharmaceutical products.

The encapsulation efficiency, which expresses the process efficiency to keep resveratrol within the carrier matrix rather than on particles surface, should also be evaluated. Result in Table 4 (~97.7%) shows that the greatest fraction of the quantified resveratrol was within the particles, entrapped by the Maillard-reacted compounds. Only the small portion placed over the surface (<3%) was more likely to be affected by environmental conditions. This result is similar to or even higher than the ones reported in previous works that employed traditional methods to produce emulsions before the spray drying, like rotor-stator and high-pressure homogenizers (Koga, Andrade, Ferruzzi, & Lee, 2016; Sanguansri et al., 2013). These traditional methods are well known for providing a very small droplet size (≤1 μm) with a more polydisperse distribution (Jafari et al., 2008b). Literature on spray drying states that the lower the oil droplet size, the higher the encapsulation efficiency (Jafari et al., 2008a; Reineccius, 2004; Soottitantawat, Yoshii, Furuta, Ohkawara, & Linko, 2003). In this sense, our results are very important because they show that, even with bigger droplet sizes (~30 μm), emulsions obtained by membrane emulsification were able to provide excellent resveratrol retention and encapsulation efficiency once submitted to spray drying process. Resveratrol interactions and/ or complexations to the encapsulating matrix are likely mechanisms that enabled such results. Previous works have demonstrated resveratrol ability to bind NaCas through hydrophobic interactions and hydrogen bonding (Acharya, Sanguansri, & Augustin, 2013; Bourassa, Bariyanga, & Tajmir-Riahi, 2013), and even suggested that resveratrol affinity for casein proteins could be higher than that for oil components (Ye, Thomas, Sanguansri, Liang, & Augustin, 2013). In this case, even with the droplet disruption caused by the atomization nozzle in the spray drying process, resveratrol was able to keep sited within the encapsulating matrix, and not over the particles surface.

Thus, membrane emulsification, known as a low-energy emulsification method, and which enables the production of much more monodisperse emulsions, with more controllable droplet size, presents itself as a very efficient emulsification method to be used in integration with spray drying, alternatively to the traditional high-energy devices.

4 Conclusions

Regarding membrane emulsification process, our work has shown that, once phases composition, membrane material, pore size and temperature are kept constant, emulsions obtained by membrane emulsification present significant decrease on droplet size upon shear stress increase, until reaching stabilization. Furthermore, the dispersed phase transmembrane flux can affect positively the droplet size. Phase composition is another key factor regarding droplet size and polydispersity: inducing the Maillard reaction to the continuous phase can increase mean droplet size compared to the emulsions stabilised by the non-reacted continuous phase. Our most important achievement was with respect to the integration between the membrane emulsification and spray drying processes. Results have showed that despite the increased mean droplet size (~30 μm) obtained for the emulsions produced in the small scale membrane system, the spray-dried powder presented high process and encapsulation efficiencies (>97%), small mean diameter (~10 μm) and water content around 3.6%. These particle properties are very similar to those of spray-dried particles obtained from emulsions produced using traditional emulsification methods in previous published works, which usually can have droplet size as fine as 1 μm or smaller. This finding shows that the integration of membrane emulsification and spray drying processes can be very efficient to produce solid microparticles for applications in food, pharmaceutical and cosmetic products. Our future work will investigate different emulsification methods combined with spray drying and their effect on particles properties, as well as an evaluation from an energy consumption perspective, to determine the advantages/disadvantages of each of the emulsification processes. Particles simulated gastrointestinal conditions should also be evaluated.

CRediT authorship contribution statement

Larissa Consoli: Conceptualization, Investigation, Formal analysis, Data curation, Writing - original draft, Visualization. **Míriam Dupas Hubinger:** Supervision, Writing - review & editing, Funding acquisition. **Marijana M. Dragosavac:** Conceptualization, Methodology, Resources, Supervision, Writing - review & editing.

Declaration of Competing Interest

The authors declare that they have no known competing financial interests or personal relationships that could have appeared to influence the work reported in this paper.

Acknowledgements

Appendix A Supplementary material

Supplementary data to this article can be found online at https://doi.org/10.1016/j.foodres.2020.109359.

References

The corrections made in this section will be reviewed and approved by a journal production editor. The newly added/removed references and its citations will be reordered and rearranged by the production team.

Acharya, D.P., Sanguansri, L., & Augustin, M.A. (2013). Binding of resveratrol with sodium caseinate in aqueous solutions. Food Chemistry, 141(2), 1050–1054. doi:10.1016/j.foodchem.2013.03.037.

Amri, A., Chaumeil, J.C., Sfar, S., & Charrueau, C. (2012). Administration of resveratrol: What formulation solutions to bioavailability limitations?. Journal of Controlled Release, 158(2), 182–193. doi:10.1016/J.JCONREL.2011.09.083.

AOAC (2005). Official Methods of Analysis of AOAC. Washington DC EUA.

Artero, A., Artero, A., Tarín, J.J., & Cano, A. (2018). The impact of moderate wine consumption on health. Maturitas, 80(1), 3–13. doi:10.1016/j.maturitas.2014.09.007.

Berendsen, R., Güell, C., & Ferrando, M. (2015). Spray dried double emulsions containing procyanidin-rich extracts produced by premix membrane emulsification: Effect of interfacial composition. Food Chemistry, 178, 251–258. doi:10.1016/J.FOODCHEM.2015.01.093.

Bhandari, B.R., Datta, N., & Howes, T. (1997). Problems associated with spray drying of sugar-rich foods. Drying Technology, 15(2), 671–684. doi:10.1080/07373939708917253.

Bourassa, P., Bariyanga, J., & Tajmir-Riahi, H.A. (2013). Binding sites of resveratrol, genistein, and curcumin with milk α- and β-caseins. The Journal of Physical Chemistry B, 117(5), 1287–1295. doi:10.1021/jp3114557.

Bouyer, E., Mekhloufi, G., Rosilio, V., Grossiord, J.-L., & Agnely, F. (2012). Proteins, polysaccharides, and their complexes used as stabilizers for emulsions: Alternatives to synthetic surfactants in the pharmaceutical field?. International Journal of Pharmaceutics, 436(1–2), 359–378. doi:10.1016/j.ijpharm.2012.06.052.

Brown, L., Kroon, P.A., Das, D.K., Das, S., Tosaki, A., Chan, V., … Feick, P. (2009). The biological responses to resveratrol and other polyphenols from alcoholic beverages. Alcoholism: Clinical and Experimental Research, 33(9), 1513–1523. doi:10.1111/j.1530-0277.2009.00989.x.

Cardoso, T., Gonçalves, A., Estevinho, B.N., & Rocha, F. (2019). Potential food application of resveratrol microparticles: Characterization and controlled release studies. Powder Technology, 355, 593–601. doi:10.1016/j.powtec.2019.07.079.

Charcosset, C. (2009). Preparation of emulsions and particles by membrane emulsification for the food processing industry. Journal of Food Engineering, 92(3), 241–249. doi:10.1016/j.jfoodeng.2008.11.017.

Chedea, V.S., Vicas, S.I., Sticozzi, C., Pessina, F., Frosini, M., Maioli, E., & Valacchi, G. (2017). Resveratrol: From diet to topical usage. Food & Function, 8(11), 3879–3892. doi:10.1039/C7FO01086A.

Chen, S., Han, Y., Jian, L., Liao, W., Zhang, Y., & Gao, Y. (2020). Fabrication, characterization, physicochemical stability of zein-chitosan nanocomplex for co-encapsulating curcumin and resveratrol. Carbohydrate Polymers, 236, 116090. doi:10.1016/j.carbpol.2020.116090.

Cheng, H., Khan, M.A., Xie, Z., Tao, S., Li, Y., & Liang, L. (2020). A peppermint oil emulsion stabilized by resveratrol-zein-pectin complex particles: Enhancing the chemical stability and antimicrobial activity in combination with the synergistic effect. Food Hydrocolloids, 103, 105675. doi:10.1016/j.foodhyd.2020.105675.

Choi, Y.K., Poudel, B.K., Marasini, N., Yang, K.Y., Kim, J.W., Kim, J.O., … Yong, C.S. (2012). Enhanced solubility and oral bioavailability of itraconazole by combining membrane emulsification and spray drying technique. International Journal of Pharmaceutics, 434(1–2), 264–271. doi:10.1016/j.ijpharm.2012.05.039.

Consoli, L., de Figueiredo Furtado, G., da Cunha, R.L., & Hubinger, M.D. (2017). High solids emulsions produced by ultrasound as a function of energy density. Ultrasonics Sonochemistry, 38, 772–782. doi:10.1016/j.ultsonch.2016.11.038.

Consoli, L., Dias, R.A.O., da Silva Carvalho, A.G., da Silva, V.M., & Hubinger, M.D. (2019). Resveratrol-loaded microparticles: Assessing Maillard conjugates as encapsulating matrices. Powder Technology, 353, 247–256. doi:10.1016/J.POWTEC.2019.04.085.

Consoli, L., Dias, R.A.O., Rabelo, R.S., Furtado, G.F., Sussulini, A., Cunha, R.L., & Hubinger, M.D. (2018). Sodium caseinate-corn starch hydrolysates conjugates obtained through the Maillard reaction as stabilizing agents in resveratrol-loaded emulsions. Food Hydrocolloids, 84, 458–472. doi:10.1016/J.FOODHYD.2018.06.017.

da Silva Carvalho, A.G., da Costa Machado, M.T., da Silva, V.M., Sartoratto, A., Rodrigues, R.A.F., & Hubinger, M.D. (2016). Physical properties and morphology of spray dried microparticles containing anthocyanins of jussara (Euterpe edulis Martius) extract. Powder Technology, 294, 421–428. doi:10.1016/j.powtec.2016.03.007.

de Oliveira, F.C., Coimbra, J.S. dos R., de Oliveira, E.B., Zuñiga, A.D.G., & Rojas, E.E.G. (2016). Food protein-polysaccharide conjugates obtained via the Maillard reaction: A review. Critical Reviews in Food Science and Nutrition, 56(7), 1108–1125. doi:10.1080/10408398.2012.755669.

Díaz-Ruiz, R., Martínez-Rey, L., Laca, A., Álvarez, J.R., Gutiérrez, G., & Matos, M. (2020). Enhancing trans-Resveratrol loading capacity by forcing W1/O/W2 emulsions up to its colloidal stability limit. Colloids and Surfaces B: Biointerfaces, 111130. doi:10.1016/j.colsurfb.2020.111130.

Donsi, F., Sessa, M., Mediouni, H., Mgaidi, A., & Ferrari, G. (2011). Encapsulation of bioactive compounds in nanoemulsion-based delivery systems. 11th International Congress on Engineering and Food (Icef11), 1, 1666–1671. doi:10.1016/j.profoo.2011.09.246.

Dragosavac, M.M., Holdich, R.G., Vladisavljević, G.T., & Sovilj, M.N. (2012). Stirred cell membrane emulsification for multiple emulsions containing unrefined pumpkin seed oil with uniform droplet size. Journal of Membrane Science, 392–393, 122–129. doi:10.1016/j.memsci.2011.12.009.

Dragosavac, M.M., Sovilj, M.N., Kosvintsev, S.R., Holdich, R.G., & Vladisavljević, G.T. (2008). Controlled production of oil-in-water emulsions containing unrefined pumpkin seed oil using stirred cell membrane emulsification. Journal of Membrane Science, 322(1), 178–188. doi:10.1016/j.memsci.2008.05.026.

Dragosavac, M.M., Vladisavljević, G.T., Holdich, R.G., & Stillwell, M.T. (2012). Production of porous silica microparticles by membrane emulsification. Langmuir, 28(1), 134–143. doi:10.1021/la202974b.

Drapala, K.P., Auty, M.A.E., Mulvihill, D.M., & O'Mahony, J.A. (2017). Influence of emulsifier type on the spray-drying properties of model infant formula emulsions. Food Hydrocolloids, 69, 56–66. doi:10.1016/j.foodhyd.2016.12.024.

Drusch, S., Serfert, Y., Scampicchio, M., Schmidt-Hansberg, B., & Schwarz, K. (2007). Impact of physicochemical characteristics on the oxidative stability of fish oil microencapsulated by spray-drying. Journal of Agricultural and Food Chemistry, 55(26), 11044–11051. doi:10.1021/jf072536a.

Duan, X., Li, M., Ma, H., Xu, X., Jin, Z., & Liu, X. (2016). Physicochemical properties and antioxidant potential of phosvitin–resveratrol complexes in emulsion system. Food Chemistry, 206, 102–109. doi:10.1016/J.FOODCHEM.2016.03.055.

Feng, J.L., Wang, Z.W., Zhang, J., Wang, Z.N., & Liu, F. (2009). Study on food-grade vitamin E microemulsions based on nonionic emulsifiers. Colloids and Surfaces A-Physicochemical and Engineering Aspects, 339(1–3), 1–6. doi:10.1016/j.colsurfa.2009.01.002.

Feng, W., Yue, C., Wusigale, Ni, Y., & Liang, L. (2018). Preparation and characterization of emulsion-filled gel beads for the encapsulation and protection of resveratrol and α-tocopherol. Food Research International, 108, 161–171. doi:10.1016/j.foodres.2018.03.035.

Gharsallaoui, A., Roudaut, G., Chambin, O., Voilley, A., & Saurel, R. (2007). Applications of spray-drying in microencapsulation of food ingredients: An overview. Food Research International, 40(9), 1107–1121. doi:10.1016/j.foodres.2007.07.004.

Gunstone, F.D. (2005). Vegetable Oils. Bailey's Industrial Oil and Fat Products (6th ed.,). Hoboken - New Jersey: John Wiley & Sons. p. 606.

Hemar, Y., Cheng, L., Oliver, C., Sanguansri, L., & Augustin, M. (2010). Encapsulation of resveratrol using water-in-oil-in-water double emulsions. Food Biophysics, 5(2), 120–127. doi:10.1007/s11483-010-9152-5.

Herrera, M.L., Falabella, C., Melgarejo, M., & Añón, M.C. (1998). Isothermal crystallization of hydrogenated sunflower oil: I—Nucleation. Journal of the American Oil Chemists' Society, 75(10), 1273–1280. doi:10.1007/s11746-998-0172-y.

Hogan, S.A., McNamee, B.F., O'Riordan, E.D., & O'Sullivan, M. (2001). Emulsification and microencapsulation properties of sodium caseinate/carbohydrate blends. International Dairy Journal, 11(3), 137–144. doi:10.1016/s0958-6946(01)00091-7.

Hogan, S.A., McNamee, B.F., O'Riordan, E.D., & O'Sullivan, M. (2001). Microencapsulating properties of sodium caseinate. Journal of Agricultural and Food Chemistry, 49(4), 1934–1938. doi:10.1021/jf000276q.

Hung, C.-F., Chen, J.-K., Liao, M.-H., Lo, H.-M., & Fang, J.-Y. (2006). Development and evaluation of emulsion-liposome blends for resveratrol delivery. Journal of Nanoscience and Nanotechnology, 6(9), 2950–2958. doi:10.1166/jnn.2006.420.

Imbrogno, A., Dragosavac, M., Piacentini, E., Vladisavljević, G.T., Holdich, R.G., & Giorno, L. (2015). Polycaprolactone multicore-matrix particle for the simultaneous encapsulation of hydrophilic and hydrophobic compounds produced by membrane emulsification and solvent diffusion processes. Colloids and Surfaces B: Biointerfaces, 135, 116–125. doi:10.1016/j.colsurfb.2015.06.071.

Jafari, S.M., Assadpoor, E., He, Y., & Bhandari, B. (2008). Encapsulation efficiency of food flavours and oils during spray drying. Drying Technology, 26(7), 816–835. doi:10.1080/07373930802135972.

Jafari, S.M., Assadpoor, E., He, Y., & Bhandari, B. (2008). Re-coalescence of emulsion droplets during high-energy emulsification. Food Hydrocolloids, 22(7), 1191–1202. doi:10.1016/j.foodhyd.2007.09.006.

Burns, J., Yokota, T., Ashihara, H., Lean, M.E.J., & Crozier, A. (2002). Plant foods and herbal sources of resveratrol. Journal of Agricultural and Food Chemistry, 50(11), 3337–3340. doi:10.1021/jf0112973.

Ji, M., Li, Q., Ji, H., & Lou, H. (2014). Investigation of the distribution and season regularity of resveratrol in Vitis amurensis via HPLC–DAD–MS/MS. Food Chemistry, 142, 61–65. doi:10.1016/j.foodchem.2013.06.131.

Kchaou, H., Benbettaieb, N., Jridi, M., Nasri, M., & Debeaufort, F. (2019). Influence of Maillard reaction and temperature on functional, structure and bioactive properties of fish gelatin films. Food Hydrocolloids, 97, 105196. doi:10.1016/j.foodhyd.2019.105196.

Koga, C.C., Andrade, J.E., Ferruzzi, M.G., & Lee, Y. (2016). Stability of trans-resveratrol encapsulated in a protein matrix produced using spray drying to UV light stress and simulated gastro-intestinal digestion. Journal of Food Science, 81(2), C292–C300. doi:10.1111/1750-3841.13176.

Kosvintsev, S.R., Gasparini, G., Holdich, R.G., Cumming, I.W., & Stillwell, M.T. (2005). Liquid−liquid membrane dispersion in a stirred cell with and without controlled shear. Industrial & Engineering Chemistry Research, 44(24), 9323–9330. doi:10.1021/ie0504699.

Lam, Y.Y., Peterson, C.M., & Ravussin, E. (2013). Resveratrol vs. calorie restriction: Data from rodents to humans. Experimental Gerontology, 48(10), 1018–1024.

Landau, L.D., & Lifshitz, E.M. (1959). Fluid mechanics (3rd ed.). Oxford, U.K.: Pergamon Press.

Li, R., Cui, Q., Wang, G., Liu, J., Chen, S., Wang, X., … Jiang, L. (2019). Relationship between surface functional properties and flexibility of soy protein isolate-glucose conjugates. Food Hydrocolloids, 95, 349–357. doi:10.1016/j.foodhyd.2019.04.030.

Maschke, A., Becker, C., Eyrich, D., Kiermaier, J., Blunk, T., & Gopferich, A. (2007). Development of a spray congealing process for the preparation of insulin-loaded lipid microparticles and characterization thereof. European Journal of Pharmaceutics and Biopharmaceutics, 65(2), 175–187. doi:10.1016/j.ejpb.2006.08.008.

Matos, M., Gutierrez, G., Coca, J., & Pazos, C. (2014). Preparation of water-in-oil-in-water (W-1/O/W-2) double emulsions containing trans-resveratrol. Colloids and Surfaces A-Physicochemical and Engineering Aspects, 442, 69–79. doi:10.1016/j.colsurfa.2013.05.065.

Matos, M., Gutiérrez, G., Iglesias, O., Coca, J., & Pazos, C. (2015). Enhancing encapsulation efficiency of food-grade double emulsions containing resveratrol or vitamin B12 ◦by membrane emulsification. Journal of Food Engineering, 166, 212–220. doi:10.1016/j.jfoodeng.2015.06.002.

Matos, M., Laca, A., Rea, F., Iglesias, O., Rayner, M., & Gutiérrez, G. (2018). O/W emulsions stabilized by OSA-modified starch granules versus non-ionic surfactant: Stability, rheological behaviour and resveratrol encapsulation. Journal of Food Engineering, 222, 207–217. doi:10.1016/J.JFOODENG.2017.11.009.

Matos, M., Suárez, M.A., Gutiérrez, G., Coca, J., & Pazos, C. (2013). Emulsification with microfiltration ceramic membranes: A different approach to droplet formation mechanism. Journal of Membrane Science, 444, 345–358. doi:10.1016/J.MEMSCI.2013.05.033.

McClements, D.J. (2005). Food emulsions. Principles, practices, and techniques (2nd ed.). Florida: CRC Press.

Morelli, S., Holdich, R.G., & Dragosavac, M.M. (2017). Microparticles for cell encapsulation and colonic delivery produced by membrane emulsification. Journal of Membrane Science, 524, 377–388. doi:10.1016/j.memsci.2016.11.058.

Morris, G.A., Sims, I.M., Robertson, A.J., & Furneaux, R.H. (2004). Investigation into the physical and chemical properties of sodium caseinate-maltodextrin glyco-conjugates. Food Hydrocolloids, 18(6), 1007–1014. doi:10.1016/j.foodhyd.2004.04.013.

Mustapha, O., Kim, K.S., Shafique, S., Kim, D.S., Jin, S.G., Seo, Y.G., … Choi, H.-G. (2017). Development of novel cilostazol–loaded solid SNEDDS using a SPG membrane emulsification technique: Physicochemical characterization and in vivo evaluation. Colloids and Surfaces B: Biointerfaces, 150, 216–222. doi:10.1016/J.COLSURFB.2016.11.039.

Nagata, S. (1975). Mixing: Principles and applications. Tokyo, Japan: Kodansha Ltd.

Nooshkam, M., Varidi, M., & Verma, D.K. (2020). Functional and biological properties of Maillard conjugates and their potential application in medical and food: A review. Food Research International. Elsevier Ltd.. doi:10.1016/j.foodres.2020.109003.

O'Dwyer, S.P., O'Beirne, D., Eidhin, D.N., & O'Kennedy, B.T. (2013). Effects of emulsification and microencapsulation on the oxidative stability of camelina and sunflower oils. Journal of Microencapsulation, 30(5), 451–459. doi:10.3109/02652048.2012.752533.

O'Regan, J., & Mulvihill, D.M. (2009). Preparation, characterisation and selected functional properties of sodium caseinate–maltodextrin conjugates. Food Chemistry, 115(4), 1257–1267. doi:10.1016/j.foodchem.2009.01.045.

Oh, D.H., Din, F.U., Kim, D.W., Kim, J.O., Yong, C.S., & Choi, H.-G. (2013). Flurbiprofen-loaded nanoparticles prepared with polyvinylpyrrolidone using Shirasu porous glass membranes and a spray-drying technique: Nano-sized formation and improved bioavailability. Journal of Microencapsulation, 30(7), 674–680. doi:10.3109/02652048.2013.774447.

Oh, D.H., Yan, Y.-D., Kim, D.W., Kim, J.O., Yong, C.S., & Choi, H.-G. (2014). Development of flurbiprofen-loaded nanoparticles with a narrow size distribution using sucrose. Drug Development and Industrial Pharmacy, 40(2), 172–177. doi:10.3109/03639045.2012.752501.

Oliver, C.M., Melton, L.D., & Stanley, R.A. (2006). Creating proteins with novel functionality via the Maillard reaction: A review. Critical Reviews in Food Science and Nutrition, 46(4), 337–350. doi:10.1080/10408690590957250.

Patel, K.R., Scott, E., Brown, V.A., Gescher, A.J., Steward, W.P., & Brown, K. (2011). Clinical trials of resveratrol. Annals of the New York Academy of Sciences, 1215(1), 161–169. doi:10.1111/j.1749-6632.2010.05853.x.

Piacentini, E., Drioli, E., & Giorno, L. (2014). Membrane emulsification technology: Twenty-five years of inventions and research through patent survey. Journal of Membrane Science, 468, 410–422. doi:10.1016/j.memsci.2014.05.059.

Piacentini, E., Giorno, L., Dragosavac, M.M., Vladisavljević, G.T., & Holdich, R.G. (2013). Microencapsulation of oil droplets using cold water fish gelatine/gum arabic complex coacervation by membrane emulsification. Food Research International, 53(1), 362–372. doi:10.1016/j.foodres.2013.04.012.

Ramakrishnan, S., Ferrando, M., Aceña-Muñoz, L., De Lamo-Castellví, S., & Güell, C. (2013). Fish oil microcapsules from O/W emulsions produced by premix membrane emulsification. Food and Bioprocess Technology, 6(11), 3088–3101. doi:10.1007/s11947-012-0950-2.

Ramakrishnan, S., Ferrando, M., Aceña-Muñoz, L., Mestres, M., De Lamo-Castellví, S., & Güell, C. (2013). Influence of emulsification technique and wall composition on physicochemical properties and oxidative stability of fish oil microcapsules produced by spray drying. Food and Bioprocess Technology, 7(7), 1959–1972. doi:10.1007/s11947-013-1187-4.

Rauf, A., Imran, M., Suleria, H.A.R., Ahmad, B., Peters, D.G., & Mubarak, M.S. (2017). A comprehensive review of the health perspectives of resveratrol. Food & Function, 8(12), 4284–4305. doi:10.1039/C7FO01300K.

Reineccius, G.A. (2004). The spray drying of food flavors. Drying Technology, 22(6), 1289–1324. doi:10.1081/DRT-120038731.

Salama, A. H. (2020, February 1). Spray drying as an advantageous strategy for enhancing pharmaceuticals bioavailability. Drug Delivery and Translational Research. Springer. https://doi.org/10.1007/s13346-019-00648-9.

Salgado, M., Rodríguez-Rojo, S., Alves-Santos, F.M., & Cocero, M.J. (2015). Encapsulation of resveratrol on lecithin and β-glucans to enhance its action against Botrytis cinerea. Journal of Food Engineering, 165, 13–21. doi:10.1016/j.jfoodeng.2015.05.002.

Sanguansri, L., Day, L., Shen, Z., Fagan, P., Weerakkody, R., Cheng, L.J., … Augustin, M.A. (2013). Encapsulation of mixtures of tuna oil, tributyrin and resveratrol in a spray dried powder formulation. Food & Function, 4(12), 1794–1802. doi:10.1039/C3FO60197H.

Santos, J., Vladisavljević, G.T., Holdich, R.G., Dragosavac, M.M., & Muñoz, J. (2015). Controlled production of eco-friendly emulsions using direct and premix membrane emulsification. Chemical Engineering Research and Design, 98, 59–69. doi:10.1016/j.cherd.2015.04.009.

Schröder, V., & Schubert, H. (1999). Production of emulsions using microporous, ceramic membranes. Colloids and Surfaces A: Physicochemical and Engineering Aspects, 152(1–2), 103–109. doi:10.1016/S0927-7757(98)00688-8.

Schubert, H., & Engel, R. (2004). Product and formulation engineering of emulsions. Chemical Engineering Research & Design, 82(A9), 1137–1143. doi:10.1205/cerd.82.9.1137.44154.

Sessa, M., Balestrieri, M.L., Ferrari, G., Servillo, L., Castaldo, D., D'Onofrio, N., … Tsao, R. (2014). Bioavailability of encapsulated resveratrol into nanoemulsion-based delivery systems. Food Chemistry, 147, 42–50. doi:10.1016/j.foodchem.2013.09.088.

Shao, P., Feng, J., Sun, P., & Ritzoulis, C. (2019). Improved emulsion stability and resveratrol encapsulation by whey protein/gum arabic interaction at oil-water interface. International Journal of Biological Macromolecules, 133, 466–472. doi:10.1016/j.ijbiomac.2019.04.126.

Shepherd, R., Robertson, A., & Ofman, D. (2000). Dairy glycoconjugate emulsifiers: Casein-maltodextrins. Food Hydrocolloids, 14(4), 281–286. doi:10.1016/s0268-005x(99)00067-3.

Silva, H.D., Cerqueira, M.A., & Vicente, A.A. (2012). Nanoemulsions for Food Applications: Development and Characterization. Food and Bioprocess Technology, 5(3), 854–867. doi:10.1007/s11947-011-0683-7.

Silva, P.S., Morelli, S., Dragosavac, M.M., Starov, V.M., & Holdich, R.G. (2017). Water in oil emulsions from hydrophobized metal membranes and characterization of dynamic interfacial tension in membrane emulsification. Colloids and Surfaces A: Physicochemical and Engineering Aspects, 532, 77–86. doi:10.1016/J.COLSURFA.2017.06.051.

Soottitantawat, A., Yoshii, H., Furuta, T., Ohkawara, M., & Linko, P. (2003). Microencapsulation by spray drying: Influence of emulsion size on the retention of volatile compounds. Journal of Food Science, 68(7), 2256–2262. doi:10.1111/j.1365-2621.2003.tb05756.x.

Spyropoulos, F., Lloyd, D.M., Hancocks, R.D., & Pawlik, A.K. (2014). Advances in membrane emulsification. Part A: Recent developments in processing aspects and microstructural design approaches. Journal of the Science of Food and Agriculture, 94(4), 613–627. doi:10.1002/jsfa.6444.

Stillwell, M.T., Holdich, R.G., Kosvintsev, S.R., Gasparini, G., & Cumming, I.W. (2007). Stirred cell membrane emulsification and factors influencing dispersion drop size and uniformity. Industrial & Engineering Chemistry Research, 46(3), 965–972. doi:10.1021/ie0611094.

Suárez, M.A., Gutiérrez, G., Coca, J., & Pazos, C. (2013). Stirred tank membrane emulsification using flat metallic membranes: A dimensional analysis. Chemical Engineering and Processing: Process Intensification, 69, 31–43. doi:10.1016/J.CEP.2013.02.005.

Takeungwongtrakul, S., Benjakul, S., & H-kittikun, A. (2015). Wall materials and the presence of antioxidants influence encapsulation efficiency and oxidative stability of micro-encapsulated shrimp oil. European Journal of Lipid Science and Technology, 117(4), 450–459. doi:10.1002/ejlt.201400235.

Vladisavljević, G.T. (2019). Preparation of microemulsions and nanoemulsions by membrane emulsification. Colloids and Surfaces A: Physicochemical and Engineering Aspects, 579, 123709. doi:10.1016/j.colsurfa.2019.123709.

Vladisavljević, G.T., Wang, B., Dragosavac, M.M., & Holdich, R.G. (2014). Production of food-grade multiple emulsions with high encapsulation yield using oscillating membrane emulsification. Colloids and Surfaces A: Physicochemical and Engineering Aspects, 458, 78–84. doi:10.1016/j.colsurfa.2014.05.011.

Vladisavljević, G.T., & Williams, R.A. (2005). Recent developments in manufacturing emulsions and particulate products using membranes. Advances in Colloid and Interface Science, 113(1), 1–20. doi:10.1016/j.cis.2004.10.002.

Wan, Z.-L., Wang, J.-M., Wang, L.-Y., Yang, X.-Q., & Yuan, Y. (2013). Enhanced physical and oxidative stabilities of soy protein-based emulsions by incorporation of a water-soluble stevioside-resveratrol complex. Journal of Agricultural and Food Chemistry, 61(18), 4433–4440. doi:10.1021/jf4003945.

Wang, J., Martínez-Hernández, A., de Lamo-Castellví, S., Romero, M.P., Kaade, W., Ferrando, M., & Güell, C. (2020). Low-energy membrane-based processes to concentrate and encapsulate polyphenols from carob pulp. Journal of Food Engineering, 281, 109996. doi:10.1016/j.jfoodeng.2020.109996.

Yang, K.Y., Hwang, D.H., Yousaf, A.M., Kim, D.-W., Shin, Y.-J., Bae, O.-N., … Choi, H.-G. (2013). Silymarin-loaded solid nanoparticles provide excellent hepatic protection: Physicochemical characterization and in vivo evaluation. International Journal of Nanomedicine, 8(1), 3333. doi:10.2147/IJN.S50683.
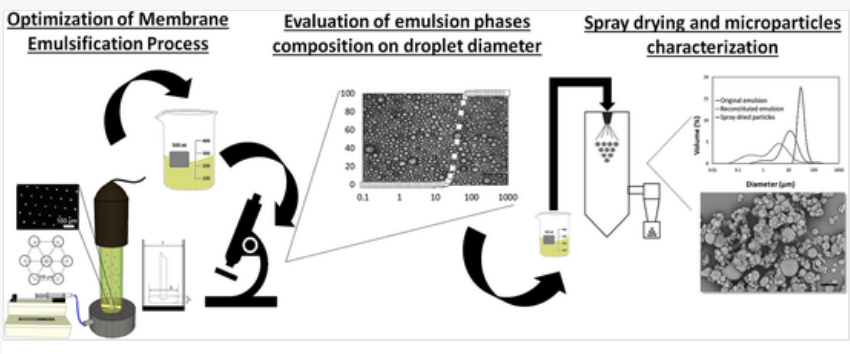
Ye, J.-H., Thomas, E., Sanguansri, L., Liang, Y.-R., & Augustin, M.A. (2013). Interaction between Whole Buttermilk and Resveratrol. Journal of Agricultural and Food Chemistry, 61(29), 7096–7101. doi:10.1021/jf401784z.

Zha, F., Dong, S., Rao, J., & Chen, B. (2019). Pea protein isolate-gum Arabic Maillard conjugates improves physical and oxidative stability of oil-in-water emulsions. Food Chemistry, 285, 130–138. doi:10.1016/j.foodchem.2019.01.151.

Zhang, F., Khan, M.A., Cheng, H., & Liang, L. (2019). Co-encapsulation of α-tocopherol and resveratrol within zein nanoparticles: Impact on antioxidant activity and stability. Journal of Food Engineering, 247, 9–18. doi:10.1016/j.jfoodeng.2018.11.021.

Zhang, X., Li, X., Liu, L., Wang, L., Massounga Bora, A.F., & Du, L. (2020). Covalent conjugation of whey protein isolate hydrolysates and galactose through Maillard reaction to improve the functional properties and antioxidant activity. International Dairy Journal, 102, 104584. doi:10.1016/j.idairyj.2019.104584.

Graphical abstract

Highlights

- Nickel membranes in a dispersion cell were used to produce oil-in-water emulsions.
- Transmembrane flux and shear stress effect on emulsions properties was investigated.
- Phases composition influence on droplet size and interfacial tension was studied.
- Resveratrol-loaded emulsions were produced with the dispersion cell and spray dried.
- Spray-dried powder had high resveratrol retention and encapsulation efficiency (>97%).

Appendix A Supplementary material

The following are the Supplementary data to this article:

[Multimedia Component 1](#)

Supplementary Data 1

Queries and Answers

Query: Your article is registered as a regular item and is being processed for inclusion in a regular issue of the journal. If this is NOT correct and your article belongs to a Special Issue/Collection please contact b.sims@elsevier.com immediately prior to returning your corrections.
Answer: It is right. It is supposed to be inserted in a regular issue.

Query: The author names have been tagged as given names and surnames (surnames are highlighted in teal color). Please confirm if they have been identified correctly.
Answer: Yes

Query: Please confirm that the provided email larissa.consoli@gmail.com is the correct address for official communication, else provide an alternate e-mail address to replace the existing one, because private e-mail addresses should not be used in articles as the address for communication.
Answer: This is the right e-mail.